

OPEN ACCESS

Forest Height Inversion Using Dual-pol Polarimetric SAR Interferometry

To cite this article: W X Fu *et al* 2014 *IOP Conf. Ser.: Earth Environ. Sci.* **17** 012072

View the [article online](#) for updates and enhancements.

You may also like

- [An efficient compressive sensing based PS-DInSAR method for surface deformation estimation](#)
J T Li, H P Xu, L Shan et al.
- [Layover and shadow detection based on distributed spaceborne single-baseline InSAR](#)
Zou Huanxin, Cai Bin, Fan Changzhou et al.
- [Potential of SAR for monitoring transportation infrastructures: an analysis with the multi-dimensional imaging technique](#)
G Fornaro, D Reale and S Verde



ECS
The
Electrochemical
Society
Advancing solid state &
electrochemical science & technology

DISCOVER
how sustainability
intersects with
electrochemistry & solid
state science research

Forest Height Inversion Using Dual-pol Polarimetric SAR Interferometry

W X Fu¹, H D Guo¹, C Xie¹, Y C Lu² and X W Li¹

¹Institute of Remote Sensing and Digital Earth, CAS, Haidian district, Beijing, 100094

²International Institute for Earth System Science, Nanjing University, Nanjing, 210093

E-mail: wxfu@ceode.ac.cn

Abstract. Polarimetric Synthetic Aperture Radar Interferometry (PolInSAR) has been extensively applied for forest parameter inversion over different frequencies and polarimetric conditions. So far, most research was based on full-pol SAR images with relatively small coverage. A spaceborne SAR system will have the potential for PolInSAR applications used for global forest monitoring. Spaceborne dual-pol SAR images usually have higher resolution and larger swath than full-pol mode. In this paper, forest height retrieval was attempted by PolInSAR from a L-band spaceborne dual-pol SAR pairs using HH and HV channels. The random volume over ground (RVoG) model was used to retrieve the height and the coherence optimization method was extended to the dual-pol PolInSAR, which makes use of polarimetry to enhance the quality of SAR interferograms. The three-stage process is also used in the dual-pol PolInSAR technique. Finally, the experimental test was performed for forest height estimation on the dual-pol L-band SAR data of the Saihanba forest acquired by the ALOS PALSAR sensor in 2009.

1. Introduction

Estimating the height of worldwide forest is crucial to help scientists better understand forests and the role they play in environment and global change [1] - [3]. Remote sensing technique is, nowadays, the most effective means to retrieve forest height at regional and global scales for its large scale and real-time characteristics. Microwave can penetrate the forest volume layer and get to the ground surface, and then the back signal contains the information of the forest vertical structure, which makes synthetic aperture radar (SAR) be potential to retrieve the forest parameters.

Polarimetric Synthetic Aperture Radar Interferometry (PolInSAR) is a technique to identify and separate the vertical scattering phase centres of the natural green forest media in polarization signal for the purpose of classification and parameters estimation. Three-stage inversion process is one of the most frequently used methods with PolInSAR data for extracting forest height [7], [8], [10].

At present, PolInSAR technique is mostly based on the full-pol SAR images. The theory foundation of PolInSAR is the random volume over ground (RVoG) model [6] which is a two-layer coherent scattering model. This model is established firstly to describe the vegetation parameters, and then the polarization and interferometry are unified by defining a complex interferometric coherence. Full-pol SAR system can provide the more information than dual-pol mode, but is usually with the lower spatial resolution and the smaller swath. In this paper, we demonstrate that the forest height is retrieved by dual-pol PolInSAR technique using L-band HH+HV channels image pairs, and finally,



we perform a preliminary experiment of dual-pol PolInSAR using ALOS PALSAR images over the Saihanba National Forest Park, in Hebei Province, China.

2. Two-layer random volume model

Two-layer random volume model was first proposed by Treuhaft [4], [9], described the forest as a volume of randomly oriented particles over a ground surface. Forest is assumed as a homogeneous volume of randomly orientated particles characterized by the constant mean extinction coefficient σ . The attenuation in the volume is modelled as an exponential function. Then the complex coherence of the random volume over ground can be expressed as

$$\begin{aligned}\hat{\gamma}(w) &= e^{i\phi_0} \frac{\hat{\gamma}_v + \mu(w)}{1 + \mu(w)} \\ &= e^{i\phi_0} \left(\hat{\gamma}_v + \frac{\mu(w)}{1 + \mu(w)} (1 - \hat{\gamma}_v) \right) \\ &= e^{i\phi_0} (\hat{\gamma}_v + L(w)(1 - \hat{\gamma}_v))\end{aligned}\quad (1)$$

w presents the variable affected by the polarization w . $\mu(w)$ is ground to volume ratio, which depends on the polarization; $L(w)$ is real non-negative, and lies in the range $0 \leq L(w) \leq 1$, with limits occurring at one end for pure volume scattering ($\mu = 0$), and at the other by pure ground scattering ($\mu = \infty$); $\hat{\gamma}_v$ is the complex coherence for the volume alone and can be expressed as

$$\hat{\gamma}_v = \frac{2\sigma}{\cos\theta_0(e^{(2\sigma h_v)/\cos\theta_0} - 1)} \int_0^{h_v} e^{ik_z z} e^{(2\sigma z)/\cos\theta_0} dz. \quad (2)$$

σ is attenuation coefficient; k_z is the wavenumber, defined as $k_z = \frac{4\pi B_\perp}{\lambda R \sin\theta_0}$.

3. Dual-pol polinsar technology

3.1. Complex coherence coefficient of PolInSAR

In a full-pol PolInSAR system, assuming reciprocal scattering, the common representation of the coherency matrix T_6 is estimated by 3-D Pauli-scattering vectors k_i which is given by

$$k_i = \frac{1}{\sqrt{2}} [S_{HHi} + S_{VV_i}, \quad S_{HHi} - S_{VV_i}, \quad 2S_{HV_i}]^T \quad (4)$$

$$T_6 = \langle k k^T \rangle = \begin{bmatrix} T_{11} & \Omega_{12} \\ \Omega_{12}^T & T_{22} \end{bmatrix} \quad \text{with } k = \begin{bmatrix} k_1 \\ k_2 \end{bmatrix} \quad (5)$$

where $i = 1, 2$ represents the interferometric image pairs, and T indicates the matrix transposition operation. S_{HHi} , S_{VV_i} and S_{HV_i} are elements of the polarimetric scattering matrices. T_{ii} corresponds to polarimetric coherency matrix of scattering vector k_i , and Ω_{12} is the polarimetric interferometry between k_1 and k_2 .

For the vector interferometry, the scattering vectors k_1 and k_2 are projected onto the normalized complex vectors w_1 and w_2 respectively, the scattering coefficients μ_1 and μ_2

$$\begin{aligned}\mu_1 &= w_1^{*T} k_1 \\ \mu_2 &= w_2^{*T} k_2\end{aligned}\quad (6)$$

where $w_i = [w_{i1} \quad w_{i2} \quad w_{i3}]^T$ represents the i th scattering mechanism.

Assuming $w_{i1} = w_{i2}$ in equation (6), the VV channel will be removed from the scattering coefficients μ_1 and μ_2 , and then they can be expressed only by the two channels HH and HV, which means that the dual-pol PolInSAR is the subspace of full-pol mode. And then the equations (4) and (6) can be simplified as

$$k_i = \sqrt{2} [S_{HHi}, \quad S_{HV_i}]^T \quad (7)$$

$$\begin{aligned}\mu_1 &= w_1^{*T} k_1 \\ \mu_2 &= w_2^{*T} k_2\end{aligned} \quad \text{with } w_i = [w_{i1}, \quad w_{i2}]^T \quad (8)$$

Same as the full-pol mode, the scalars can be interpreted as the complex scattering coefficients for the scattering mechanisms μ_1 and μ_2 . This notation allows us to express the interferometric coherence as follow

$$\gamma = \frac{\langle \mu_1 \mu_2^* \rangle}{\sqrt{\langle \mu_1 \mu_1^* \rangle \langle \mu_2 \mu_2^* \rangle}} = \frac{\langle w_1^{*T} [\Omega_{12}] w_2 \rangle}{\sqrt{\langle w_1^{*T} [T_{11}] w_1 \rangle \langle w_2^{*T} [T_{22}] w_2 \rangle}} \quad (9)$$

with $0 \leq |\gamma| \leq 1$. Where * means complex conjugation and $\langle \rangle$ indicates the expectation value.

3.2. Coherence optimization

The purpose of the optimization is to find the polarimetric scattering mechanisms w_1 and w_2 that make $|\gamma|$ maximum. For the dual-pol complex coherence coefficient defined in equation (9), and according to [4], [5], the optimization problem can be inverted to the eigenvalue equations.

$$\begin{aligned} [T_{11}]^{-1} [\Omega_{12}] [T_{22}]^{-1} [\Omega_{12}]^{*T} w_1 &= v w_1 \\ [T_{22}]^{-1} [\Omega_{12}]^{*T} [T_{11}]^{-1} [\Omega_{12}] w_2 &= v w_2 \end{aligned} \quad (10)$$

The two 2×2 matrices in (10) are still not Hermitian, but have real nonnegative eigenvalues. w_1 and w_2 are 2×1 vectors, which can generate the maximum and minimum optimal coherences.

4. Experimental results

We selected the Saihanba National Forest Park, located in Hebei Province, China, as the test area. The extent from east to west is about 23 km, and about 8 km from south to north, and the altitude from 1010 m to 1500 m. The trees in this park are somewhat homogeneous, including larch, spruce and Lodgepole pine, and so on.

In this study, two dual-pol ALOS PALSAR images were acquired over the Saihanba Forest Park on Jun. 24 and Aug. 9, 2009 respectively. ALOS PALSAR worked on L-band with the center wavelength 23.6 cm. For the long wavelength, the signal can penetrate the forest canopy and even reach to the ground surface, and the returns of polarizations include different volume and ground information. The location of this Park and the polarimetric σ^0 map of the dual-pol PALSAR data are shown in Figure 1.

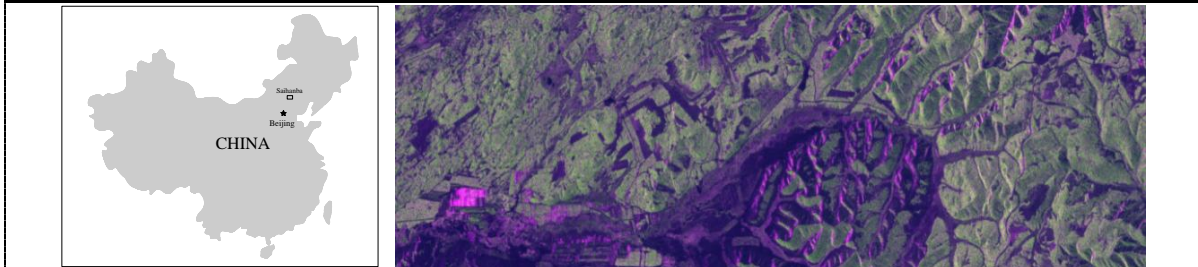


Figure 1. (Left) Location of the Saihanba National Forest Park; (Right) Polarimetric σ^0 map of the dual-pol PALSAR data, and the RGB coding: Red color corresponds to the intensity of HH backscattering, green to HV, and blue to HH-HV.

The coherences of the interferometry generated by HH-HH, HV-HV and the two optimum scattering mechanisms, we used a 3×3 average window to reduce the interferometric phase variation. The coherence maps of the HH-HH, HV-HV, and the two optimum mechanisms are shown in Figure 2 and 3.

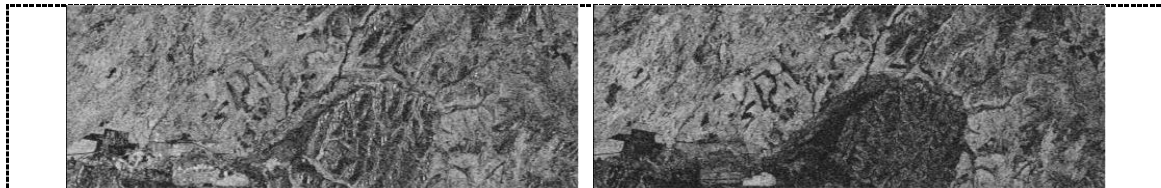
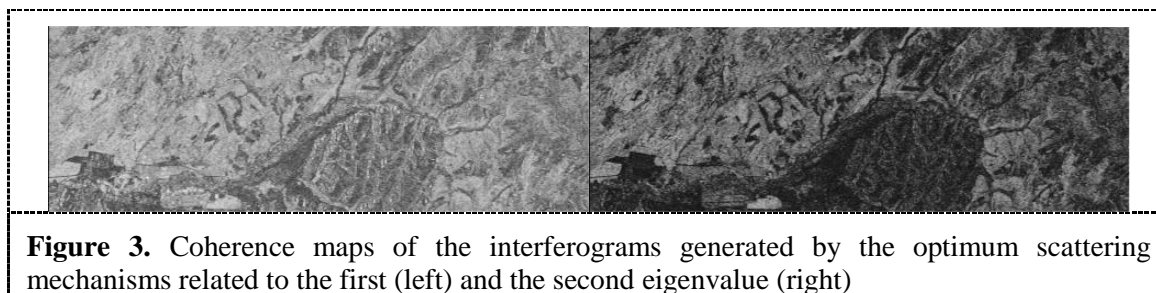
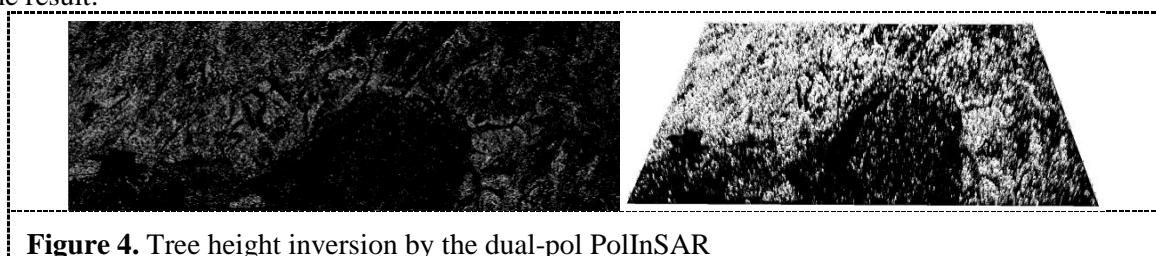


Figure 2. Coherence maps of the interferograms generated by HH and HV channels (Left: HH-HH. Right: HV-HV)



5. Result and conclusions

The tree height was retrieved by the dual-pol PolInSAR technique, which shows the potential of this technique for the tree height inversion (Figure 4). And in next work, we will analysis the accuracy of the result.



Dual-pol PolInSAR technique by the HH and HV channels is still effective for forest parameters retrieval with higher resolution and larger swath. However less information than the full-pol mode makes the linear regression process based on only the complex coherence with HH, HV channels and the corresponding optimum scattering mechanisms. For the L-band and homogeneous forest, the complex coherence points are not large dispersion from the regression line, the effect of the fewer channels still can be accepted.

In the other hand, the temporal decorrelation should also be considered in the repeat pass system, especially the time interval is large. The coherence with temporal decorrelation is expressed as

$$\tilde{\gamma} = e^{i\phi}(\gamma_t \tilde{\gamma}_v + L(w)(1 - \gamma_t \tilde{\gamma}_v)) \quad (11)$$

The SAR system on co-flying two satellites in a close formation will reduce the temporal decorrelation, which enable highly accurate interferometric measurement. In additional, for the longer wavelength such as spaceborne P band SAR system, the ionosphere effect must be considered.

Acknowledgments

This study was supported by the National Key Technology R&D Programs (2012BAC16B01, 2012BAH27B05).

6. References

- [1] Fang J, Chen A, Peng C, Zhao S and Ci L 2001 *Science*. **292** 2320 -2322
- [2] Houghton R A 2005 *Global Change Biology*. **11** 945-958
- [3] Mette T, Papathanassiou K, Hajnsek I, Pretzsch H and Biber P 2004 *Proc. IGARS*. **1** 269- 272
- [4] Papathanassiou K P and Cloude S R 2001 *IEEE Trans. Geosci. Remote Sens.* **39** 2352-2363
- [5] Cloude S R and Papathanassiou K P 1998 *IEEE Trans. Geosci. Remote Sens.* **36** 1551-1565
- [6] Garestier F, Dubois-Fernandez P and Champion I 2008 *IEEE Trans. Geosci. Remote Sens.* **46** 3544-3559
- [7] Mette T, Papathanassiou K and Hajnsek I 2004 *Proc. IGARSS*. **1** 511 – 514
- [8] Guillaso S, Reigber A and Ferro-Famil L 2005 *Proc. IGARSS*. **1** 32-35
- [9] Treuhaft R N and Siqueira P 2000 *Radio Sci.* **35** 141-177
- [10] Cloude S R and Papathanassiou K P 2003 *IEE Proc. Radar Sonar Navig.* **I50** 125-134